Journal of Alloys and Compounds 513 (2012) 328–333

Contents lists available at SciVerse ScienceDirect

Journal of Alloys and Compounds

journal homepage: www.elsevier.com/locate/jallcom

Enhanced thermoelectric performance in p-type $Ca_{0.5}Ce_{0.5}Fe_{4-x}Ni_xSb_{12}$ skutterudites by adjusting the carrier concentration

Gangjian Tan, Shanyu Wang, Yonggao Yan, Han Li, Xinfeng Tang*

State Key Laboratory of Advanced Technology for Materials Synthesis and Processing, Wuhan University of Technology, Wuhan 430070, China

ARTICLE INFO

Article history:
Received 30 July 2011
Received in revised form 7 October 2011
Accepted 10 October 2011
Available online 24 October 2011

Keywords:
p-type filled skutterudites
Ni substitution
Carrier concentration
Thermoelectric properties

ABSTRACT

Polycrystalline p-type Ca/Ce co-filled skutterudites $Ca_{0.5}Ce_{0.5}Fe_{4-x}Ni_xSb_{12}$ ($0 \le 0 \le 0.7$) compounds have been successfully prepared by traditional melting-annealing-spark plasma sintering (SPS) method. The effective adjustment in carrier concentration dominates electronic transport behavior in a manner of significant decrease of electrical conductivity as well as the enhancement in Seebeck coefficient with increasing Ni-substitution, resulting in a slight degradation of power factor. Meanwhile, the thermal conductivity, dominated by electronic contribution, decreases monotonically with increasing Ni-substitution, and the negligible mass fluctuation between Ni and Fe gives rise to a slight change in phonon thermal conductivity. In particular, the lattice thermal conductivity of these co-filled skutterudites shows rather low value compared with other double filled analogs due to the large difference in localized frequencies between Ca and Ce elements. Due to the opposite tendency between electronic properties and thermal conductivities, *ZT* governed by carrier concentration increases firstly and then decreases. The maximum *ZT* value of 0.85 at 700 K is obtained in the sample $Ca_{0.5}Ce_{0.5}Fe_{3.5}Ni_{0.5}Sb_{12}$ with a carrier concentration of $\sim 2.6 \times 10^{20}$ cm^{-3}, and this peak value is comparable to some excellent p-type skutterudites reported so far. This study demonstrates that the effective control in carrier concentration can be easily realized through proper Fe-site substitutions without deterioration in carrier mobility and change in electronic structure, thus bringing about an optimization of thermoelectric figure of merit.

1. Introduction

In times of energy shortage thermoelectric (TE) power generation is an attractive issue for recovering electrical power directly from waste heat, for instance in automotive exhaust systems or solar energy converters [1–3]. The main limit of thermoelectricity to niche applications is the low efficiency of current TE materials. The efficiency of TE materials is governed by the dimensionless figure of merit $ZT = \alpha^2\sigma T/\kappa$, where α is the Seebeck coefficient, σ is the electrical conductivity, T is the absolute temperature, and κ is the total thermal conductivity, which contains both electronic and lattice contribution κ_C and κ_L, respectively.

Skutterudites, having attracted great interest for decades because of their low-cost and promising TE performance, are some of the most promising candidates for TE power generation at moderate temperature [4,5]. Truly, n-type skutterudites, possessing large effective masses and thus high power factors, have extensively obtained high *ZT*s exceeding 1.4 in double or triple filling system owing to the drastic decrease in lattice contribution to thermal transport [6–12]. P-type skutterudites based mainly on $FeSb_3$ [13–17] and being essential to module fabrications, however, exhibit relatively low *ZT*s for their low values of Seebeck coefficients. Therefore it is of great importance to improve the thermoelectric performances of p-type skutterudites which is tricky and needs to touch upon some fundamental physical issues.

As mentioned previously, the three parameters determining *ZT* are closely related to the carrier concentration, and thus effective control in carrier concentration is crucial to obtain a high power factor and thus improved figure of merit. In p-type $FeSb_3$-based skutterudites, the intrinsic high carrier density leads to poor TE performance and the substitution in Fe sublattice is a widely adopted and effective approach [18–21]. Generally, Ni or Co is considered to be a typical choice and also extensively studied. In comparison with Co, Ni is more efficacious and each atom donates two electrons, realizing an effective control in carrier density.

Besides substitution at cation site, filling in the nanocages by rare earth, alkali or alkaline earth metal element is actually becoming popular to form a so-called filled skutterudites [6–17,22,23]. The main benefit of filling atoms is the introduction of excessive scattering to heat transport phonons originated from the "rattling" effect in the local structures. This strategy has truly witnessed great achievement in the past decade. In order to greatly depress κ_L,

* Corresponding author. Tel.: +86 027 87662832.
E-mail address: tangxf@whut.edu.cn (X. Tang).

0925-8388/$ – see front matter.
doi:10.1016/j.jallcom.2011.10.042

however, the kind and fraction of filling atoms need to be carefully considered. It has been found out that different kinds of filler atoms with distinct vibration frequencies in the voids can decrease the lattice thermal conductivity largely exceeding alloying limit [6,7,24,25]. In particular, as compared to other double filled skutterudites, Ca and Ce co-filled systems display the lowest κ_L value especially when the filling fraction of Ca and Ce is approximately identical [26]. This benefit is mainly attributed to the large difference of vibration frequencies between the two atoms. So, in this research, we choose Ca and Ce as fillers and their filling fraction is both fixed at 0.5. The aim of the present work is to realize an effective control in carrier concentration by Ni substitution at Fe site, and thus well regulate the electrical transport properties (*PF*) while retaining a low κ_L in Ca–Ce double filling system. Consequently an overall improvement in *ZT* can be expected

2. Experiment

Polycrystalline samples with nominal compositions $Ca_{0.5}Ce_{0.5}Fe_{4-x}Ni_xSb_{12}$ (x = 0, 0.1, 0.3, 0.5 and 0.7) were prepared as follows. Stoichiometric quantities of the constituent pure elements Ca (99.9%, ingot), Ce (99.99%, plate), Fe (99.999%, shot), Ni (99.999%, ingot), and Sb (99.9999%, ingot) were weighed according to their nominal composition, loaded into a quartz tube with carbon depositing on the inner wall, and sealed under a pressure of 10^{-3} Pa. All the above procedures were done in a glove box filled with high-purity Ar (O_2 < 0.1 ppm, H_2O < 5 ppm). The samples were slowly heated to 1373 K and rested for 24 h. They were then quenched in a saltwater base and annealed at 953 K for 168 h. The resulting ingots were ground into fine powders and then sintered by spark plasma sintering (SPS) at 853 K for 5 min under pressure of 40 MPa.

The phase compositions of bulk samples were determined by powder X-ray diffraction (XRD) (PANalytical X'Pert Pro X-ray diffraction) using Cu Kα radiation (λ = 1.5406 Å). The chemical compositions of the samples were analyzed by inductively coupled plasma Auger emission spectroscopy (ICP-AES). ICP analysis confirms that the actual composition is very close to the nominal composition. Hence, in this paper, the nominal compositions will be used for all samples. Electrical conductivity (σ) and Seebeck coefficient (α) were simultaneously measured by commercial equipment (ZEM-1, Ulvac Riko, Inc.) under a low pressure inert gas (He) atmosphere from 300 K to 800 K. The thermal conductivity (κ) was calculated from the measured thermal diffusivity (D), specific heat (C_p), and density (d) using the relationship $\kappa = D \times C_p \times d$. The thermal diffusivity was tested by the laser flash diffusivity method using a Netzsch LFA 457 system and the specific heat (C_p) was measured by TA instrument: DSC Q20. All the measurements were performed in the temperature range from 300 K to 800 K. The densities of the bulk samples were measured by the Archimedes method and the relative densities of obtained bulk samples are higher than 98.0%. The Hall coefficient (R_H) and electrical conductivity (σ_H) at room temperature were measured by Accent HL5500PC Hall system using the van der Pauw method with the magnetic field strength of 0.513 T, and the corresponding carrier concentration (n) and carrier mobility (μ_H) were calculated by the followed equations: $n = 1/e|R_H|$ and $\mu_H = \sigma/ne$.

3. Results and discussion

3.1. Phase compositions

Fig. 1(a) shows the powder XRD patterns of $Ca_{0.5}Ce_{0.5}Fe_{4-x}Ni_xSb_{12}$ (x = 0, 0.1, 0.3, 0.5, 0.7) compounds after SPS. The XRD patterns demonstrate that the major phase is $CoSb_3$ (JCPDS No. 51-0824) for all samples, which is crystallized in a cubic $CoAs_3$-type structure with $Im3$ group. As the Ni nominal composition increases upon 0.7, at 2θ = 31.274°, a small peak can be observed which corresponds to the NiSb (1 0 1) peak (PDF No. 02-0783). This indicates that the solubility limit of Ni is less than 0.7 in the compounds. The enlarged (6 0 0) peaks of the XRD patterns shown in Fig. 1(b) display an apparent shift to high angle with increasing the Ni content, which is mainly due to the smaller atomic radius of Ni (1.62 Å) compared with that of iron (1.72 Å). This also presumably verifies that the Ni atoms successfully enter into the crystal lattice of the compounds. However, it can be noted that there is no obvious peak shift for the samples with Ni content larger than 0.5, indicating that the solubility limit of Ni in Fe site is around 0.5.

3.2. Electrical transport properties

Fig. 2 shows the temperature dependences of electrical transport properties for the prepared bulk materials $Ca_{0.5}Ce_{0.5}Fe_{4-x}Ni_xSb_{12}$. The electrical conductivities decrease monotonically with increasing temperature which indicates a degenerate semiconductor characteristic. Moreover, the electrical conductivity decreases with increasing the Ni content. Conversely, the Seebeck coefficient exhibits an opposite variation tendency. In order to further investigate the detailed transport properties of the prepared bulk samples, the room temperature Hall coefficients were measured, as well as the corresponding carrier concentrations and mobilities were calculated.

As shown in Fig. 3(a), the carrier concentration decreases with increasing the Ni content. Since Ni owns two outmost electrons more than Fe, Ni doping at Fe site would donate electrons into the system and thus lower the hole concentration. In fact, for filled skutterudites, one can evaluate the carrier concentration by estimating the effective hole numbers (N) in a unit cell using a simple charge counting method. For $Ca_{0.5}Ce_{0.5}Fe_{4-x}Ni_xSb_{12}$ skutterudites, fillers, such as Ca and Ce, would donate their valence electrons to the framework and the effective charge states were reported to be around +3 and +2, respectively [26–28]. Since Fe (Ni) is one electron less (more) than Co, the effective charge state of Fe (Ni) in skutterudites should be close to −1 (+1). Therefore, N is equal to (1.5–2x). Positive value of (1.5–2x) indicates the major carrier is holes, while negative value suggests electrons as the major carrier. For example, in $Ca_{0.5}Ce_{0.5}Fe_{3.5}Ni_{0.5}Sb_{12}$ sample, $N = (1.5 - 2 \times 0.5) = 0.5 > 0$, hence it shows p-type conduction. Moreover, the larger N, the higher hole concentration can be expected. Fig. 3(b) reveals the experimental Hall carrier concentration as a function of Ni content x. Apparently, experimental Hall carrier concentration increases with increasing N. So, with the increasing Ni content x, N decreases, thereby lowering the hole concentration.

The composition dependence of carrier mobility is plotted in Fig. 3(c) and shows a nonmonotonic variation. The hole mobility slightly increases when Fe is substituted by a small amount of Ni (x = 0.1). Similar observations were also noted for Ni-substituted $CoSb_3$, such as $Ba_yCo_{4-x}Ni_xSb_{12}$ or $Ca_yCo_{4-x}Ni_xSb_{12}$ system [29–31]. However, with further increase of x, the mobility decreases gradually owing to the reinforced defect scattering caused by the differences in atomic mass, size and electronegativity between Ni and Fe. Based on equation $\sigma = pe\mu_H$, it is not difficult to understand that the variations of p and μ co-affect the varying of electrical conductivity.

To further understand the mechanisms of the variation of Seebeck coefficient, by assuming a charge carrier scattering distance independent of energy and degenerate approximation, the Seebeck coefficient can be written as Eq. (1) [32,33]:

$$\alpha = \frac{\pi}{3}\frac{k_B^2 T}{e}\frac{d\ln(\sigma)}{d\ln(E)}| = \frac{8\pi^2 k_B^2}{3eh^2} m^* T \left(\frac{\pi}{3p}\right)^{2/3} \quad (1)$$

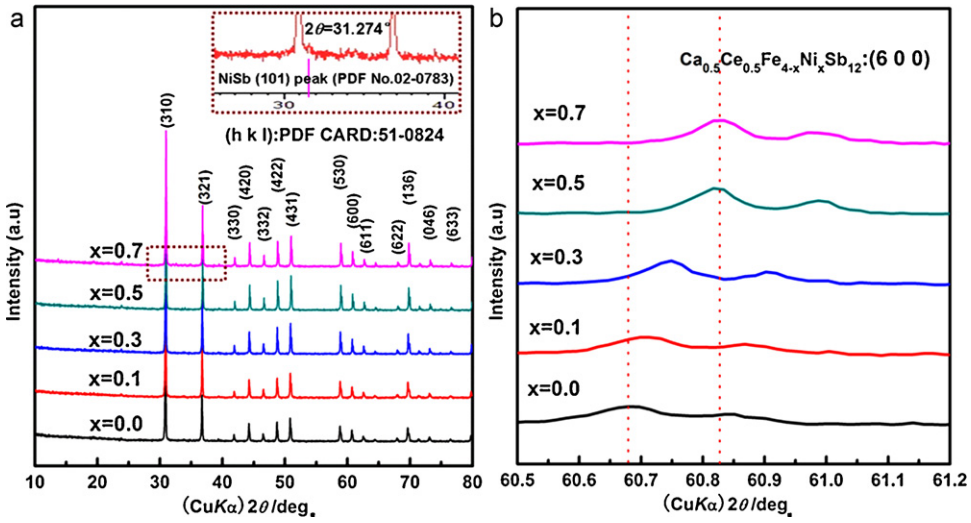

Fig. 1. (a) The powder XRD patterns and (b) enlarged (6 0 0) peaks of XRD patterns for the $Ca_{0.5}Ce_{0.5}Fe_{4-x}Ni_xSb_{12}$ ($0 \le 0 \le 0.7$) compounds. The inset patterns in (a) are the local enlargement of the patterns for the sample with $x = 0.5$.

where k_B, E_F, h, m^*, and T are the Boltzmann constant, Fermi energy, Planck constant, effective hole mass and absolute temperature, respectively. The relationship of room temperature α-p is presented in Fig. 3(d) and the solid line demonstrates a $p^{-2/3}$ dependence which indicates that the dominant scattering mechanism in $Ca_{0.5}Ce_{0.5}Fe_{4-x}Ni_xSb_{12}$ bulk samples is acoustic phonon scattering [32], which can be also demonstrated in other p-type filled skutterudites [34]. Hence, the change of the Seebeck coefficient is predominated by the variation of carrier concentration.

The power factors for all compounds are presented in Fig. 4(a). It can be noted that with increasing the Ni content, the power factor slightly decreases. The variation of the *PF* can be well interpreted by the theory proposed by Ioffe [35], Goldsmid [36] and Slack [2]: the weighed mobility $U = (m^*)^{3/2}\mu$, depending solely on the effective mass m^* and mobility μ of the carrier, could be used to approximately characterize the electrical transport properties of a TE material.

Based on Fermi statistics in a single parabolic-band model, Seebeck coefficient α and hole concentration p are given by [8,37–39]:

$$\alpha = \frac{k_B}{e}\left[\frac{(2+r)F_{1+r}(\eta)}{(1+r)F_r(\eta)} - \eta\right] \quad (2)$$

Table 1
The carrier effective masses m^*, calculated weighed mobilities U and Lorenz constants L at 300 K for the $Ca_{0.5}Ce_{0.5}Fe_{4-x}Ni_xSb_{12}$ ($x = 0, 0.1, 0.3, 0.5, 0.7$) compounds.

x	m^* (m_e)	U/cm^2 V^{-1} s^{-1}	L/10^{-8}V^2/K^2
0	0.76	26.3	2.00
0.1	0.74	21.9	1.98
0.3	0.80	23.4	1.92
0.5	0.82	23.5	1.84
0.7	0.81	17.4	1.77

$$p = \sqrt{\frac{2}{\pi}}\left[\frac{m^* k_B T}{\hbar^2}\right]^{3/2} F_{1/2}(\eta) \quad (3)$$

where r is the exponent of the energy dependence of the hole mean-free-path, m^* is the hole effective mass, e is the electron charge, $\eta = E_F/k_BT$ is the reduced Fermi energy, E_F is the Fermi Energy, k_B is Boltzmann constant, and F_x is the Fermi integral of order x. As mentioned above, holes are mainly scattered by acoustic phonons, so we suppose $r = 0$. The estimated m^* is between 0.74 and 0.82 m_e (m_e is the free electron mass), nearly independent of Ni content (see Table 1). Subsequently, the weighed mobility was calculated according to the calculated m^* and measured μ

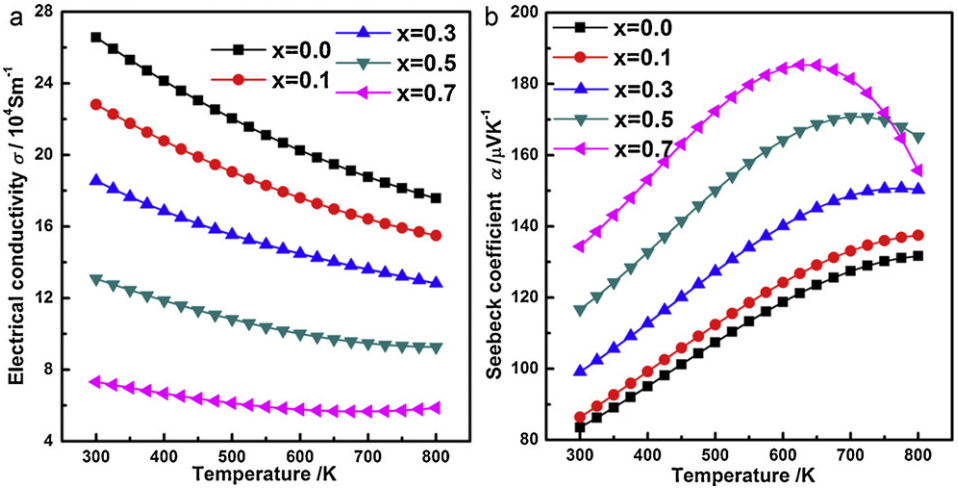

Fig. 2. The temperature dependences of the electrical properties for the $Ca_{0.5}Ce_{0.5}Fe_{4-x}Ni_xSb_{12}$ ($0 \le 0 \le 0.7$) compounds. (a) Seebeck coefficient. (b) Electrical conductivity.

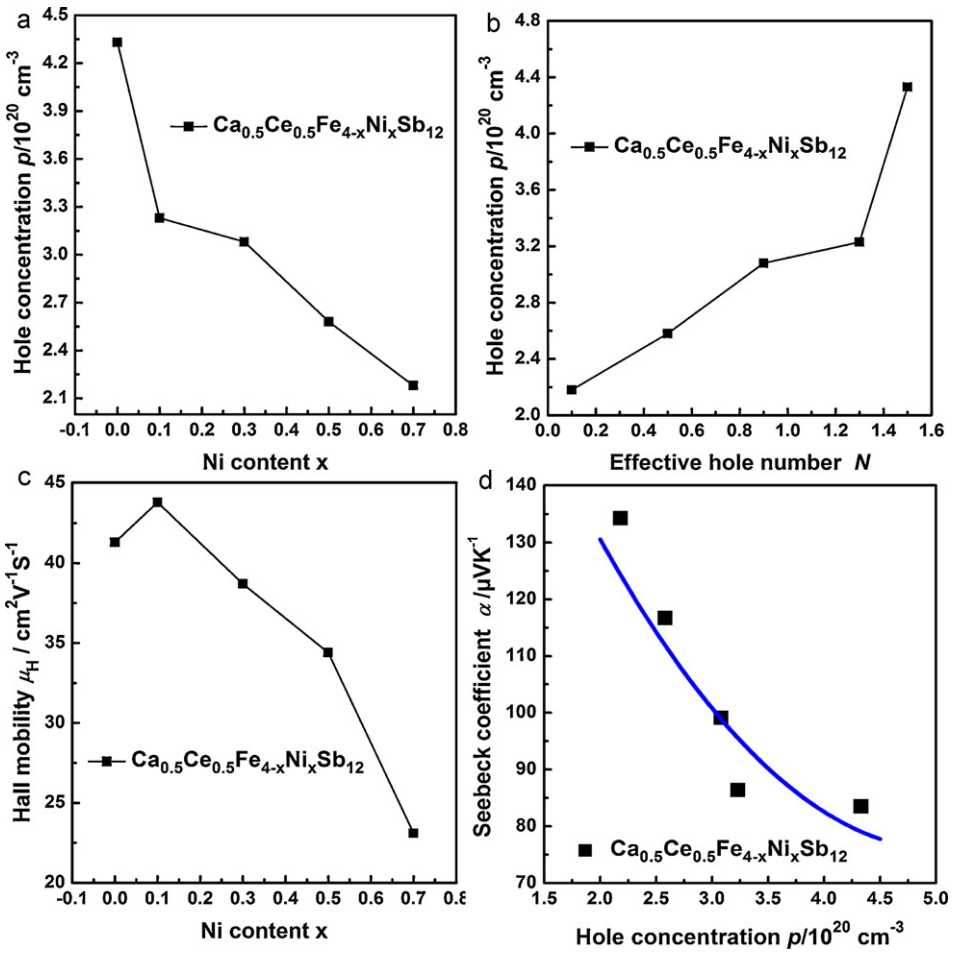

Fig. 3. (a) Room temperature carrier concentrations p as a function of x; (b) the experimental Hall carrier concentration p as a function of Ni content x; (c) carrier motilities μ_H as a function of x; (d) the room temperature Seebeck coefficients as a function of carrier concentration and the solid line demonstrates such an $p^{-2/3}$ dependence for the bulk $Ca_{0.5}Ce_{0.5}Fe_{4-x}Ni_xSb_{12}$ ($0 \le 0 \le 0.7$) samples.

from the Hall data. The room temperature weighed mobility (U) and power factor (PF) as a function of Ni substitution amount x are plotted in Fig. 4(b). The U and PF show the same trend with the change of x, and one can conclude that the slight deterioration of PF mainly arises from the decreasing trend of the mobility.

3.3. Thermal transport properties and ZTs

The temperature dependences of thermal transport properties for $Ca_{0.5}Ce_{0.5}Fe_{4-x}Ni_xSb_{12}$ compounds are presented in Fig. 5. As shown in Fig. 5(a), with increasing temperature, the thermal conductivities for all samples first remain unchanged and then increase

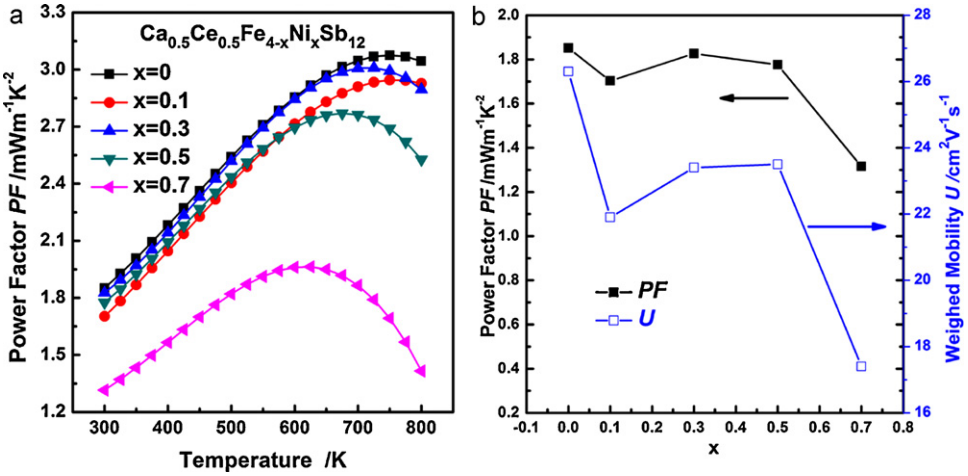

Fig. 4. (a) The temperature dependences of power factors; (b) The room temperature weighed mobilities (U) and power factors (PF) as a function of nickel substitution amount x for the bulk $Ca_{0.5}Ce_{0.5}Fe_{4-x}Ni_xSb_{12}$ ($0 \le 0 \le 0.7$) compounds.

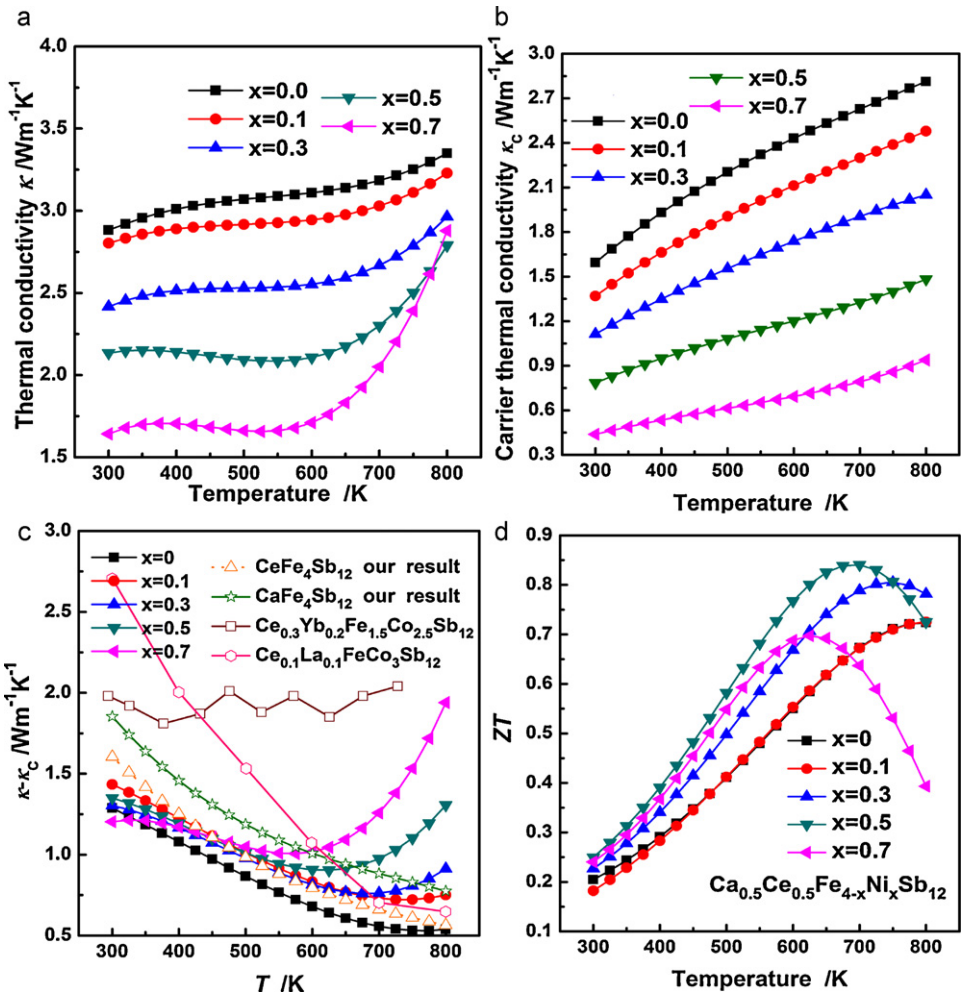

Fig. 5. The temperature dependences of the thermal transport properties for the $Ca_{0.5}Ce_{0.5}Fe_{4-x}Ni_xSb_{12}$ ($0 \le 0 \le 0.7$) compounds. (a) Thermal conductivity, (b) carrier thermal conductivity, (c) lattice thermal conductivity. The lattice thermal conductivities for the samples $CaFe_4Sb_{12}$ and $CeFe_4Sb_{12}$ are from our unpublished results. For comparison, the lattice thermal conductivities as a function of temperature for Ce–Yb [44] and Ce–La [45] double filled systems are incorporated in (c). (d) The temperature dependences of *ZT* values for all the samples.

at elevated temperature owing to the bipolar diffusion carriers conducting much heat. Fig. 5(b) displays the temperature dependence of carrier thermal conductivity κ_C calculated according to the Wiedemann–Franz equation:

$$\kappa_C = L\sigma T \tag{4}$$

where σ is the measured electrical conductivity, T is the absolute temperature. The Lorenz number L can be calculated by the formula as follow [40]:

$$L = \left(\frac{k_B}{e}\right)^2 \left[\frac{3F_0(\eta)F_2(\eta) - 4F_1^2(\eta)}{F_0^2(\eta)}\right] \tag{5}$$

With the reduced Fermi energy η obtain from Eq. (2), the values are calculated to be in the range from 2.00 to $1.77 \times 10^{-8}\ V^2\ K^{-2}$ as listed in Table 1. It can be concluded from Fig. 5(b) that κ_C decreases with increasing x value mainly resulting from the decrease in electrical conductivity. The temperature dependent κ–κ_C is shown in Fig. 5(c). The values of κ–κ_C start to increase sharply especially for those with higher Ni content at high temperature between 550 K and 750 K. This can be attributed to the so-called bipolar diffusion. However, the values are almost independent of Ni substitution amount before bipolar diffusion (when we can simply rewrite κ–κ_C as κ_L, which represents lattice thermal conductivity). The same phenomenon is also observed by other researchers [39]. This seems to be contradictory to the common knowledge that the lattice thermal conductivity can be greatly reduced by alloy scattering which is supposed to strongly scatter the heat transport phonons. Mangersnes et al. [41] predicted the crystal structure, thermodynamic stability and electronic structure of 75 filled and unfilled P-based skutterudite compounds $M_xCo_{4-y}Fe_yP_{12}$ from periodic density functional calculations. They found that the rattling amplitude of the filling atom *M*, which is important for the thermal conductivity of the compounds, depends mostly on the type of filling elements and only to a small extent on the filling fraction, or the fraction of Fe in the structure. The conclusion may be also correct for Ni substituted antimony based skutterudites. What's more, Rotter et al. [42] investigated the lattice dynamics of $CoSb_3$ using inelastic X-ray scattering and they found that the low frequency phonons mainly correspond to vibrations of Sb atoms rather than Co atoms. Therefore, doping at Sb-site is believed to be more effective to scatter phonons than doping at Co-site, which has been also demonstrated by Qiu et al. [43]. Hence, we conclude that the variety and nature of the filling atoms are dominant in the lattice thermal conductivities of as-prepared samples. For comparison, the lattice thermal conductivities of some other single or double filled p-type skutterudites are also drawn in Fig. 5(c). One can see that Ca and Ce co-filled skutterudites possess the lowest lattice thermal

conductivities, which is mainly owing to the striking differences in atomic mass, size and electronegativity between Ca and Ce atoms, thus resulting in a so-called dual frequency resonant scattering [7].

The dimensionless figure of merit is calculated by the measured values of α, σ and κ and shown in Fig. 5(d). The *ZT*s first increase almost linearly with increasing temperature and reach peaks at high temperature, and then tend to decrease with further elevating temperature due to the detrimental bipolar effect. Ca and Ce co-filling makes the system exhibit a much lower κ_L. Simultaneously, Ni-doping effectively adjusts the hole concentration, and thus cooperatively regulates the electrical (*PF*) and thermal (κ_C) transport properties. Hence, all the Ni-doping samples show much higher *ZT* values compared with that of Ni-free sample resulting from decreased κ_C and high *PF*. The best *ZT* value of 0.85 at 700 K is obtained for the sample $Ca_{0.5}Ce_{0.5}Fe_{3.5}Ni_{0.5}Sb_{12}$, which is ~18% higher than that of Ni free sample.

4. Conclusions

In this work, a traditional melting-annealing-spark plasma sintering method is successfully utilized to synthesize p-type Ni-substituted and Ca and Ce co-filled skutterudite compounds $Ca_{0.5}Ce_{0.5}Fe_{4-x}Ni_xSb_{12}$ ($0 \le 0 \le 0.7$). Ni substitution effectively regulates the hole concentration and enhances the Seebeck coefficient, thereby retaining a high power factor. Simultaneously, the thermal conductivity shows a low value in Ca–Ce double filled skutterudite due to the large difference in rattling frequency. As a result, the maximum *ZT* value reaches ~0.85 at 700 K for the sample with $x = 0.5$ and a carrier concentration of $\sim 2.6 \times 10^{20}$ cm^{-3}, about 18% improvement compared with that of Ni free sample. This study demonstrates that, by carefully selecting fillers with appropriate difference in rattling frequency, the thermoelectric performance in p-type skutterudites can be properly improved through adjusting the carrier concentration.

Acknowledgments

This work was partially supported by the National Basic Research Program of China (grant no. 2007CB607501) and the Natural Science Foundation of China grant nos. 50672118 and 50731006) along with 111 Project (grant no. B07040).

References

[1] T.M. Tritt, Science 283 (1999) 804–805.
[2] G.A. Slack, CRC Handbook of Thermoelectrics, CRC Press, Boca Raton, 1995.
[3] D.M. Rowe (Ed.), CRC Handbook of Thermoelectrics, From Nano to Macro, Taylor & Francis, Boca Raton, 2006.
[4] C. Uher, Proceedings of the 21st International Conference on Thermoelectrics, IEEE, Piscataway, NJ, 2001, pp. 35–41.
[5] L.D. Chen, Z. Xiong, S.Q. Bai, J. Inorg. Mater. 25 (2010) 00561–00568.
[6] X. Shi, H. Kong, C.P. Li, C. Uher, J. Yang, J.R. Salvador, H. Wang, L. Chen, W. Zhang, Appl. Phys. Lett. 92 (2008) 182101.
[7] J. Yang, W. Zhang, S.Q. Bai, Z. Mei, L.D. Chen, Appl. Phys. Lett. 90 (2007) 192111.
[8] S.Q. Bai, Y.Z. Pei, L.D. Chen, W.Q. Zhang, X.Y. Zhao, J. Yang, Acta Mater. 57 (2009) 3135–3139.
[9] J.R. Salvador, J. Yang, H. Wang, X. Shi, J. Appl. Phys. 107 (2010) 043705.
[10] W.Y. Zhao, P. Wei, Q.J. Zhang, C.L. Dong, L.S. Liu, X.F. Tang, J. Am. Chem. Soc. 131 (2009) 3713–3720.
[11] H. Li, X.F. Tang, Q.J. Zhang, C. Uher, Appl. Phys. Lett. 94 (2009) 102114.
[12] X. Shi, J. Yang, J.R. Salvador, M.F. Chi, J.Y. Cho, H. Wang, S.Q. Bai, J.H. Yang, W.Q. Zhang, L.D. Chen, J. Am. Chem. Soc. 133 (2011) 7837–7846.
[13] D.T. Morelli, G.P. Meisner, J. Appl. Phys. 77 (2006) 3777–3781.
[14] K. Nouneh, A.H. Reshak, S. Auluck, I.V. Kityk, R. Viennois, S. Benet, S. Charar, J. Alloys Compd. 437 (2007) 39–46.
[15] D. Bérardan, C. Godart, E. Alleno, St. Berger, E. Bauer, J. Alloys Compd. 351 (2003) 18–23.
[16] G. Rogl, A. Grytsiv, P. Rogl, E. Bauer, M. Zehetbauer, Intermetallics 19 (2011) 546–555.
[17] P.F. Qiu, J. Yang, R.H. Liu, X. Shi, X.Y. Huang, G.J. Snyder, W. Zhang, L.D. Chen, J. Appl. Phys. 109 (2011) 063713.
[18] G. Rogl, A. Grytsiv, E. Bauer, P. Rogl, M. Zehetbauer, Intermetallics 18 (2010) 394–398.
[19] G. Rogl, A. Grytsiv, P. Rogl, E. Bauer, M.B. Kerber, M. Zehetbauer, S. Puchegger, Intermetallics 18 (2010) 2435–2444.
[20] G. Rogl, A. Grytsiv, E. Bauer, P. Rogl, M. Zehetbauer, Intermetallics 18 (2010) 57–64.
[21] L. Yang, J.S. Wu, L.T. Zhang, J. Alloys Compd. 364 (2004) 83–88.
[22] P.X. Lu, F. Wu, H.L. Han, Q. Wang, Z.G. Shen, X. Hu, J. Alloys Compd. 505 (2010) 255–258.
[23] A. Harnwunggmoung, K. Kurosaki, Y. Ohishi, H. Muta, S. Yamanaka, J. Alloys Compd. 509 (2011) 1084–1089.
[24] V. Keppens, D. Mandrus, B.C. Sales, B.C. Chakoumakos, P. Dai, R. Coldea, M.B. Maple, D.A. Gajewski, E.J. Freeman, S. Bennington, Nature 395 (1998) 876–878.
[25] R.P. Hereman, R.J. Jin, W. Schweika, F. Grandjean, D. Mandrus, B.C. Sales, G.J. Long, Phys. Rev. Lett. 90 (2003) 135505.
[26] X.F. Tang, H. Li, Q.J. Zhang, M. Niino, T. Goto, J. Appl. Phys. 100 (2009) 123702.
[27] X. Shi, W. Zhang, L.D. Chen, J. Yang, C. Uher, Phys. Rev. B 75 (2007) 235208.
[28] X.F. Tang, L.D. Chen, J. Wang, Q.J. Zhang, T. Goto, T. Hirai, J. Alloys Compd. 394 (2005) 259–264.
[29] J.S. Dyck, W. Chen, J. Yang, G.P. Meisner, C. Uher, Phys. Rev. B 65 (2002) 115204.
[30] J.S. Dyck, W. Chen, C. Uher, L. Chen, X. Tang, T. Hirai, J. Appl. Phys. 91 (2002) 3698–3705.
[31] M. Puyet, A. Dauscher, B. Lenoir, M. Dehmas, C. Stiewe, E. Müller, J. Hejtmanek, J. Appl. Phys. 97 (2005) 083712.
[32] P. Pichanusakorn, P. Bandaru, Mater. Sci. Eng. R 67 (2010) 19–63.
[33] F. Gascoin, S. Ottensmann, D. Stark, S.M. Haile, G.J. Snyder, Adv. Funct. Mater. 15 (2005) 1860–1864.
[34] R. Liu, X. Chen, P. Qiu, J. Liu, J. Yang, X. Huang, L. Chen, J. Appl. Phys. 109 (2011) 023719.
[35] A.F. Ioffe, Semiconductor Thermoelements and Thermoelectric Cooling, Infosearch, London, 1957.
[36] H.J. Goldsmid, Thermoelectric Refrigeration, Plenum, New York, 1964.
[37] B.C. Sales, D. Mandrus, R.K. Williams, Science 272 (1996) 1325–1328.
[38] Y.Z. Pei, S.Q. Bai, X.Y. Zhao, W. Zhang, L.D. Chen, Solid State Sci. 10 (2008) 1422–1428.
[39] J. Yang, G.P. Meisner, C.J. Rawn, H. Wang, B.C. Chakoumakos, J. Martin, G.S. Nolas, B.L. Pedersen, K. Stalick, J. Appl. Phys. 102 (2007) 083702.
[40] G.S. Nolas, J. Sharp, H.J. Goldsmid, in: A. Zunger, R. Hull, R.M. Osgood, H. Sakaki (Eds.), Thermoelectrics: Basic Principles and New Materials Developments, Springer, New York, 2001, pp. 43–76.
[41] K. Mangersness, O.M. Lóvvik, Ø. Prytz, New J. Phys. 10 (2008) 053004.
[42] M. Rotter, P. Rogl, A. Grytsiv, W. Wolf, M. Krisch, A. Mirone, Phys. Rev. B 77 (2008) 14430.
[43] P.F. Qiu, X. Shi, X.H. Chen, X.Y. Huang, R.H. Liu, L.D. Chen, J. Alloys Compd. 509 (2011) 1101–1105.
[44] K. Yang, H. Cheng, H.H. Hng, J. Ma, J.L. Mi, X.B. Zhao, T.J. Zhu, Y.B. Zhang, J. Alloys Compd. 467 (2009) 528–532.
[45] Q.M. Lu, J.X. Zhang, X. Zhang, Y.Q. Liu, D.M. Liu, M.L. Zhou, J. Appl. Phys. 98 (2005) 106107.